JOURNAL OF MATERIALS SCIENCE 37 (2002) 935–940

The radial reinforcement of the wood structure and its implication on mechanical and fracture mechanical properties—A comparison between two tree species

A. REITERER*, I. BURGERT, G. SINN, S. TSCHEGG
Institute of Meteorology and Physics, University of Agricultural Sciences Vienna, Türkenschanzstraße 18, A-1180 Vienna, Austria
E-mail: alexander.reiterer@fff.co.at

The radial direction of wood is reinforced by an additional tissue called rays. These rays are one of the reasons for the anisotropy of wood in the transverse plane. In this paper the influence of rays on the mechanical properties like tensile strength as well as on fracture mechanical parameters like critical stress intensity factor and specific fracture energy is shown. By investigating two deciduous tree species with a similar wood structure in general but a different ray characteristic in particular the importance of this radial reinforcement of the wood structure could be demonstrated. The relevance for the living tree is discussed.

1. Introduction

Wood can be generally described as an orthotropic material with three main directions [1, 2] and excellent mechanical properties in spite of its low density [3, 4]. The wood fibres are oriented in the longitudinal direction (L), their cell wall structure is optimized to provide sufficient mechanical properties regarding the main loading conditions of the living tree (e.g. bending of the stem due to wind loads). In the transverse plane the radial (R) and the tangential (T) direction can be distinguished. The mechanical properties of wood in these directions are an order of magnitude lower compared to the longitudinal direction. Therefore, the radial and the tangential direction are often not distinguished by means of their mechanical performance. However, the radial properties are significantly higher than the tangential ones. One reason is seen in the cell geometry in the radial-tangential plane [5], another follows the fact that an additional tissue called rays regarding to its radial orientation reinforces the radial direction. The ray tissue consists of parenchymatic living cells. Therefore, in most cases only the physiological functions are mentioned. Few studies have been carried out on mechanical properties of rays directly [6–9] or ray properties have been derived from the mechanical behaviour of the entire wood in relation to its anatomical characteristic [10–13]. However, each of these investigations has been focused on single mechanical parameters of the ray tissue. By integrating mechanical and fracture mechanical investigations in the transverse plane the reinforcing character of the ray tissue can be captured in a more general sense. Thus, in this paper two deciduous tree species with a similar wood structure in general but with a different ray characteristic in particular were compared regarding their transverse behaviour.

2. Materials and methods

2.1. Material characteristic

The comparison of mechanical and fracture mechanical properties was carried out on oak (*Quercus robur* L.) and ash (*Fraxinus exelsior* L.). Both trees are ring-porous species, in terms of their structural biological characterisation. Each growth ring consists of a less dense earlywood dominated by large vessels serving for water transport and a latewood dominated by fibres serving for the longitudinal stiffness and strength of the wood in the living tree. A parameter of significant structural difference between the both tree species can be found in the ray tissue characteristic. While ash consists of rather unique multiseriate and sturdy rays, for oak two types of rays can be distinguished; only a few very large rays with a height of 1 mm or more and a high amount of very small uniseriate rays (Fig. 1; images in Fig. 4).

2.2. Mechanical and anatomical measurements

In order to investigate mechanical properties of the two tree species in the transverse plane tensile strength tests were carried out. For both species wet wood samples (above fibre saturation point) of two trees were

Present Address: Austrian Industrial Research Promotion Fund (FFF), Kärntner Straße 21-23, A-1015 Vienna, Austria.

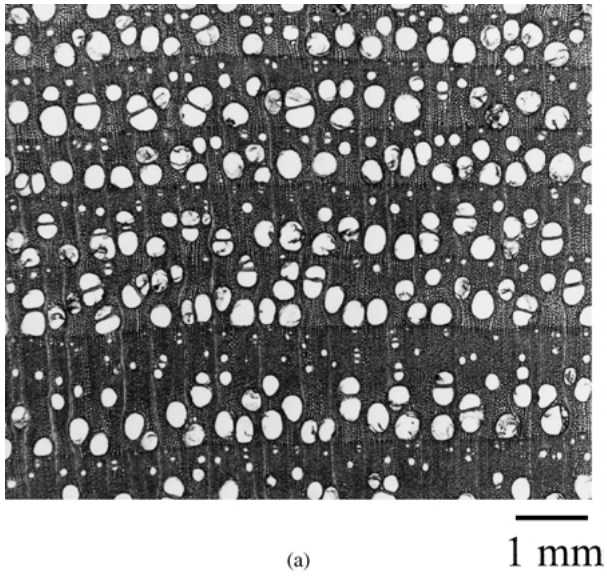

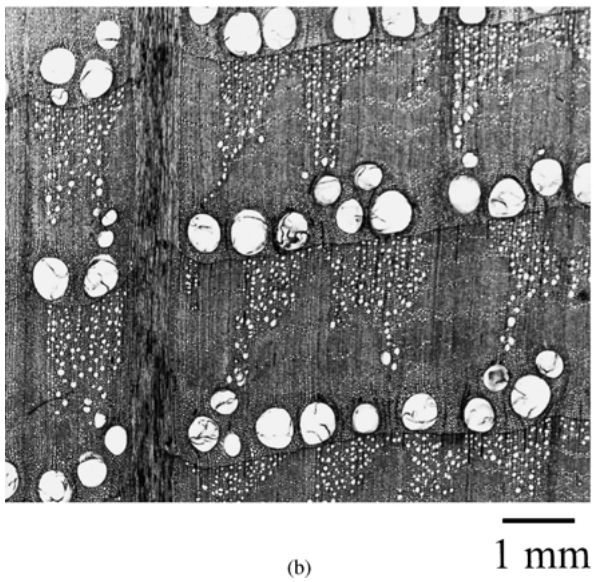

Figure 1 Cross sections of ash (a) and oak (b).

investigated. Specimens $60 \times 15 \times 15$ mm^3 in size, were prepared for radial strength tests (ray tissue oriented parallel to the force) and tangential strength tests (ray tissue oriented perpendicular to the force). The samples were tapered in their centre to a size of about 10×10 mm^2 to obtain a fracture zone far from the clamping appliance. For each tree and direction 50 samples were measured.

The wood structure had been characterised by means of density and ray abundance. For all samples the mean density (Raumdichtezahl) was determined. Since the density of the earlywood of oak and ash is much lower than the density of their latewood additionally intra-annual density profiles were measured on specimens with a moisture content of 12%, in particular to find characteristic earlywood densities (named as min. density in Fig. 5). In order to investigate the parameters of ray structure, tangential slices were prepared for an image analysis system. Every fifth sample of the tensile strength tests was measured. Next to the volume fraction of rays, their shape, number, and size were determined.

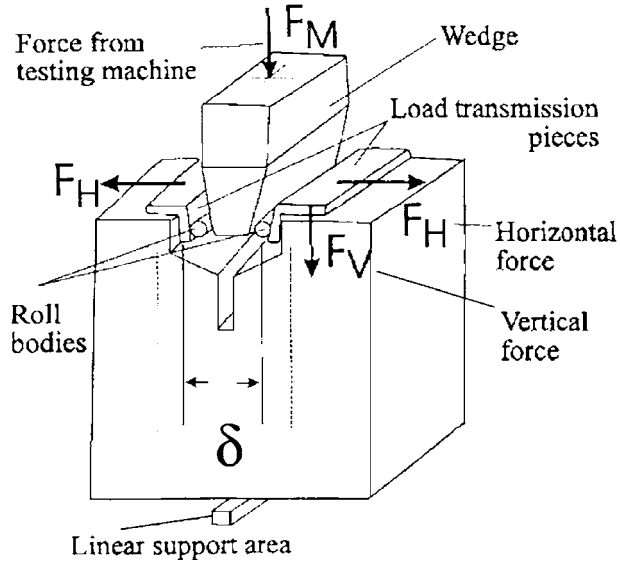

Figure 2 Testing arrangement of the wedge splitting test.

2.3. Fracture mechanical measurements

Additionally fracture mechanical parameters were determined on the same species but on different trees. Parameters characterizing Mode I fracture behaviour in the radial-longitudinal plane (RL) and the tangential-longitudinal plane (TL) were examined on dry wood (12% moisture content) of one tree of both species. For each orientation and species 10 samples were measured. The specimens had a height of 13 cm, a width of 10 cm, a thickness of 4 cm, and a notch length of 0.5 cm. In order to characterize the Mode I fracture behaviour the wedge splitting technique according to [14] was used. This method has several advantages like a favourable ratio of specimen weight to ligament area and a simple and stiff loading equipment [15] and has been used for the fracture characterization of wood [16–18]. The principle of the method is shown in Fig. 2. A wedge is pressed against load transmission pieces in a standard material testing machine, the friction being minimized by the use of roll bodies. From the measurement of the force of the testing machine F_M the horizontal splitting force F_H can be determined according to

$$F_H = F_M/2 \tan(\alpha/2) \quad (1)$$

where α is the wedge angle. A wedge angle of 18° was used in this study. The crack mouth opening displacement δ is measured by inductive displacement gauges mounted directly on the specimens on both sides of the starter notch.

The measured load-displacement curve characterizes the fracture process. The initital slope of the load-displacement curves in the linear elastic region k_{init} is determined in order to characterize the elastic behaviour. The area under the load-displacement curve divided by the fracture area A yields the specific fracture energy G_f according to

$$G_f = \frac{1}{A} \int_0^{\delta \max} F_H(\delta)\, d\delta \quad (2)$$

TABLE I Elastic parameters (elastic moduli E_i, shear moduli G_{ij} and Poisson ratios v_{ij}) of oak and ash used for the finite element simulations (values adapted from [20, 21])

	Oak	Ash
E_L [GPa]	13	15.8
E_R [GPa]	1.6	1.5
E_T [GPa]	0.9	0.8
G_{LT} [GPa]	0.8	0.6
G_{LR} [GPa]	1.2	0.9
v_{LT} [1]	0.3	0.3
v_{LR} [1]	0.3	0.3

This quantity is a "toughness" quantity characterizing the entire Mode I fracture process until the specimen is split into two halves and does not depend on specimen size and shape if the specimen size is not too small. The used size is large enough to obtain size independent values [16].

In order to characterize the maximum stress state the critical stress intensity factor K_{Ic} was determined considering the orthotropic nature of wood. The maximum horizontal splitting forces were taken as input data for a two-dimensional finite element simulation using the ANSYS©software package. The stresses at the crack tip were modeled using quarter point elements as suggested in [16, 19]. The stress intensity factors were calculated from the node displacements according to

$$\begin{pmatrix} K_I \\ K_{II} \end{pmatrix} = \sqrt{\frac{\pi}{8L}}\,\mathbf{B}^{-1} \begin{pmatrix} 4(u_B - u_{B'}) - (u_C - u_{C'}) \\ 4(v_B - v_{B'}) - (v_C - v_{C'}) \end{pmatrix} \tag{3}$$

where u_B, $u_{B'}$, u_C, $u_{C'}$ are node displacements in x direction and v_B, $v_{B'}$, v_C, $v_{C'}$ are node displacements in y-direction and L is the element length. The matrix **B** depends on the stiffness matrices of the wood species (for details see [19]). The elastic parameters used for the stiffness matrices are shown in Table I. They were adapted from the literature [20, 21] in such a way that the initial slope of the experiments could be reproduced.

3. Results

In Fig. 3 the tangential and radial strengths of the four trees were combined with the mean densities of the samples. Ash B has the lowest and ash A the highest density while the both oak trees belong to the middle. The differences in density of the both ash trees are related to their different growth ring width. While ash B shows extremely thin growth rings, ash A has very wide ones. Since the earlywood layer thickness is constant, wider growth rings contain relatively more latewood and therefore a higher mean density is measured for fast-growing ring-porous trees. The both oak trees appear very similar in their mechanical behaviour, whereas the ash trees show distinct differences. Ash B has a slightly higher strength in the tangential as well as in the radial direction compared to the oak trees. For ash A, however, the tangential strength is slightly higher whereas the radial strength of ash A is approx. 60% higher than the radial strength of the other trees.

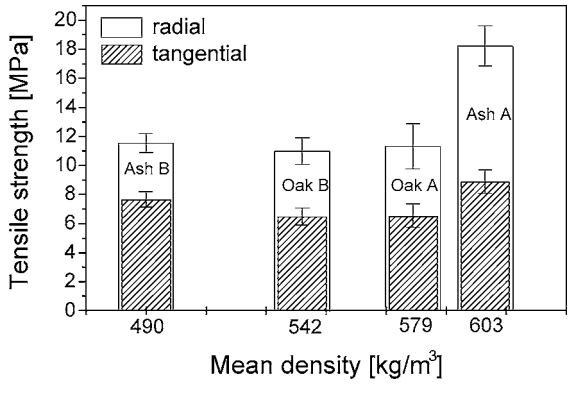

Figure 3 Radial and tangential tensile strength of oak and ash. Mean density values of the trees are scaled.

In order to examine up to a certain point these results are related to the mean densities additionally the density of the earlywood layers were investigated since the specimens fail in the earlywood layer when stressed in the radial direction. One can see in Fig. 4 that the minimum density (earlywood density) of ash A is not higher compared to the earlywood densities of ash B and the oak trees. Therefore, the higher radial strength of ash A can not be explained in case of density.

The ray structure was characterised in terms of ray volume fracture, ray shape, ray size, and number (Fig. 4). Since oak trees have two different kind of rays (very large and multiseriate rays as well as small and uniseriate rays) the parameters have to be classified. However the oak trees are very similar in their ray structure. Therefore both trees are represented by a tangential slice of only one tree, but in two magnifications, while for ash a tangential slice of each tree is shown.

The ray volume fractions of the oak trees are only slightly different, whereas the ash trees show large differences. On closer inspection of the ray number, and the ray size of the ash trees, it becomes obvious that the higher volume fraction of rays in ash A depends on an increased size of each of them, but not on a higher number of rays. However the shape of the rays is consistent in both trees.

In Fig. 5 the results of the initial slope k_{init}, the critical Mode I stress intensity factor K_{Ic} and the specific fracture energy G_f are shown. The initial slope k_{init} is characteristic for the elastic properties and proportional to an effective modulus of elasticity [22]. As specimen geometry and size was the same for all wood species and orientations the inital slopes can be compared. The stiffness in the RL system is higher than in the TL system for both species. Ash shows higher initial slopes. For the TL system the differences between the wood species are clearly lower. The ratio between the systems is slightly higher for ash. In general, the initial slopes vary from 2.5 to 3.5 N/m in the RL system and from 1.3 to 1.6 N/m in the TL system (Fig. 5a).

From the maximum splitting forces the critical stress intensity factor K_{Ic} was determined considering the orthotropic nature of wood. The finite element simulation yielded the results shown in Fig. 5b. Again the results are generally higher for ash than for oak and the differences between the two crack propagation systems are

Ash		$\bar{x}$	s	V
Density		[g/cm^3]	[g/cm^3]	[%]
tangential	A	0.591	0.030	5.1
	B	0.495	0.024	4.9
radial	A	0.615	0.034	5.5
	B	0.485	0.029	6.0
min. density	A	0.474	0.044	9.2
	B	0.450	0.028	6.3
Ray fraction		[%]	[%]	[%]
radial	A	26.37	2.45	13.1
	B	11.97	0.81	6.2
Ray number		[-]	[-]	[%]
radial	A	235	15.01	6.4
	B	235	6.15	2.6

Oak		$\bar{x}$	s	V
Density		[g/cm^3]	[g/cm^3]	[%]
tangential	A	0.567	0.04	7.1
	B	0.532	0.017	3.2
radial	A	0.59	0.02	3.4
	B	0.551	0.021	3.8
min. density	A	0.516	0.034	6.7
	B	0.447	0.021	4.7
Ray fraction		[%]	[%]	[%]
radial	A	17.50	3.04	17.3
	B	21.80	1.94	8.9
Big rays	A	6.51	2.22	34.1
	B	7.62	2.01	26.4

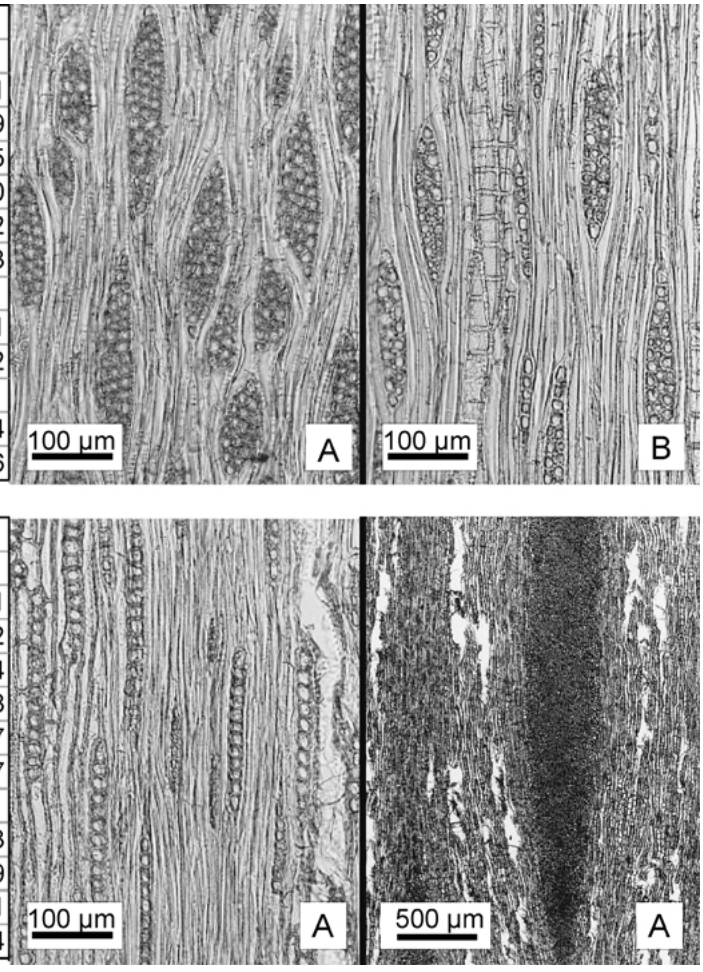

Figure 4 Anatomical parameters of both trees (A and B) of ash and oak. Representative images of the ray structure of ash A and B and oak A (first picture) with a magnification of 100 : 1; second picture of oak A in a magnification of 20 : 1.

higher for ash. Oak reaches 0.84 MPam$^{1/2}$ in the RL and 0.41 MPam$^{1/2}$ in the TL system, Ash shows values of 1.16 MPam$^{1/2}$ in the RL and 0.65 MPam$^{1/2}$ in the TL system.

The results for the specific fracture energy, characterizing the whole fracture process until complete separation of the specimen in two halves and therefore including crack initiation and propagation yield that ash has the highest specific fracture energy in both propagation systems (Fig. 5c). For oak the values are very similar (350 J/m^2 in the RL and 270 J/m^2 in the TL system) whereas for ash the difference between the systems is much greater (550 J/m^2 in the RL and 345 J/m^2 in the TL system).

An anatomical characterization of the oak and ash samples used for the fracture mechanical experiments has not been performed in detail. Nevertheless, simple microscopic inspection showed that the oakwood can be considered to be rather similar to the one used for the mechanical experiments. The anatomical characteristic of the wood of the used ash tree was in accordance with ash A by means of annual ring width and volume fraction of rays. Moreover, the measured mean density was rather similar compared with the samples for mechanical testing for oak and ash A.

The difference between the systems can be seen well on the fracture surfaces. Ash serves as an example. In Fig. 6a a typical Scanning Electron Microscope picture of the fracture surface in the RL system is shown. A multiseriate ray in the middle of the picture has been cut by the crack front. In comparison, Fig. 6b depicts the fracture surface in the TL system. A ray seperated and cut is visible.

4. Discussion

Both tree species show distinct differences of mechanical and fracture mechanical properties between the radial and tangential direction. These findings are in agreement with observations by several authors [12, 23, 24].

With regard to the elastic properties three structural features have to be distinguished in order to explain this anisotropy between the radial and tangential direction. Firstly, the annual ring structure leads to the fact that the earlywood layers and latewood layers appear in series for deformation in the tangential but in parallel for deformation in the radial direction. The second approach can be derived from the cell geometry in the radial-tangential plane [5] and the third approach follows the influence of the ray tissue [6, 12]. It can be expected that these features also influence the strength and fracture properties. In this study, two ring-porous deciduous trees with a rather similar longitudinal structure have been investigated. Therefore, the influence of the radially oriented ray tissue could be examined very well. A schematic drawing of typical features of the anatomy of ring-porous hardwoods is shown in Fig. 7 (adopted from [25], modified).

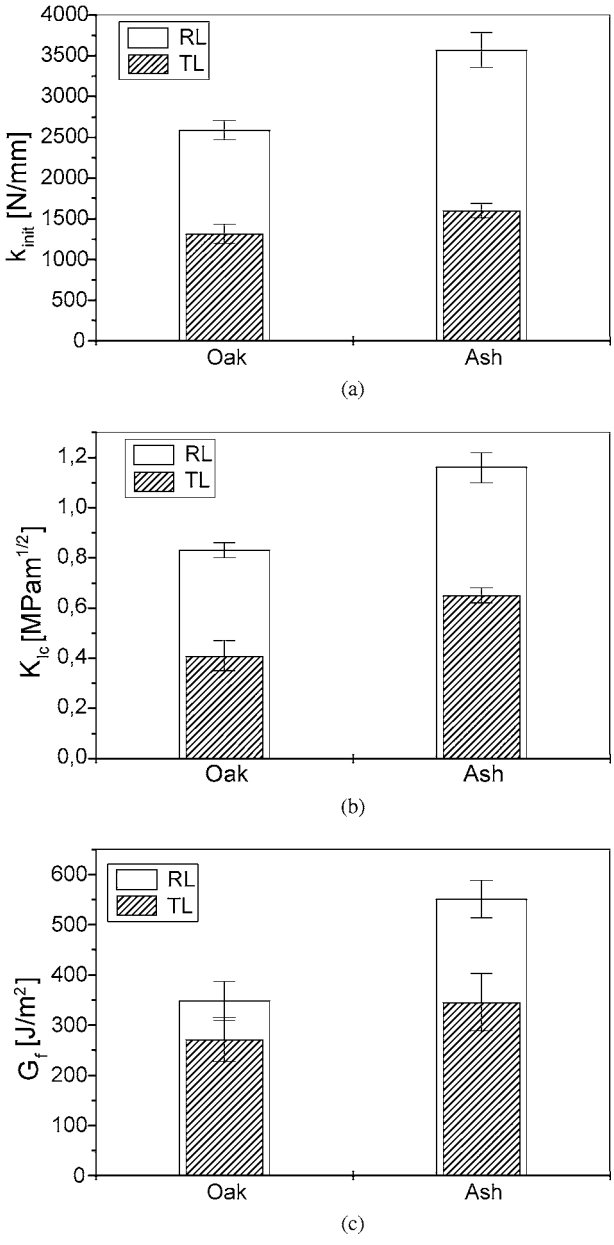

Figure 5 Inital slope k_{init} (a), critical stress intensity factor K_{Ic} (b) and specific fracture energy G_f (c) in the RL and TL crack propagation system.

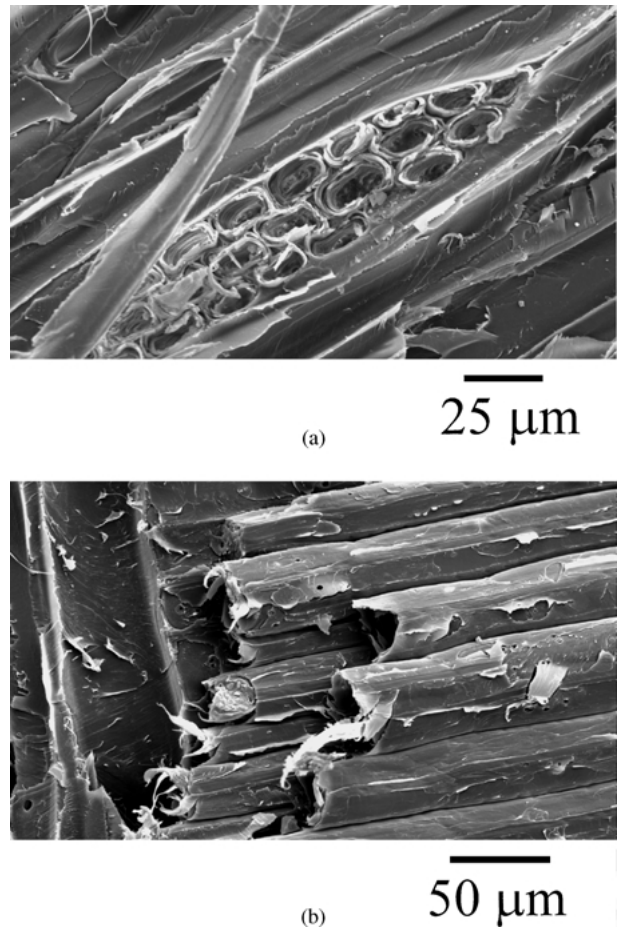

Figure 6 SEM pictures of the fracture surface of ash in the RL (a) and TL (b) crack propagation system.

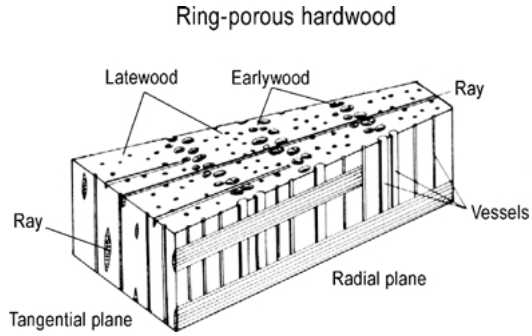

Figure 7 Schematic drawing of typical features of the anatomy of ring-porous hardwoods (adopted from [25], modified).

The both oak trees are rather similar in their tensile strength properties, whereas the both ash trees show distinct differences in particular in the radial direction. For comprehension of the mechanical properties the individual structure characteristic of each tree has to be taken into consideration. Two stepwise approaches were followed. The first was to examine the relationship to the density as an integrating parameter of structural features. However the mean density itself provides only a few information. Taking additionally the earlywood density into consideration it becomes obvious that the high radial strength of ash A can not be explained by an integrating parameter like density.

The second was to proof the relevance of different tissue proportions. In this context the volume fraction of the radial oriented ray tissue and their shape seem to be closely related to the radial mechanical properties. With increasing ray volume fraction the difference between the radial and tangential tensile strengths becomes bigger. Ash A shows the highest radial tensile strength and the highest volume fraction of rays by far. Therefore it can be stated that in the tangential direction the volume fraction of rays seems to be of less effect. However in the radial direction the volume fraction of rays influences the mechanical properties obviously.

In correspondence to the results of the mechanical investigations the rays act as a reinforcement in the RL crack propagation system. In consequence they have to carry tensile stresses in the developing process zone (containing microcracks and irreversible deformed regions) around the crack tip before macrocrack initiation as well as during the crack propagation phase when the process zone is redeveloped and running through the material. Moreover, it is most likely that the rays build fibre bridges behind the actual crack tip consuming additional fracture energy. As the ratio

between RL and TL system is higher for the K_{Ic} values compared with the specific fracture energies one may conclude that the crack initiation phase is influenced more than the propagation phase. In general the same trend is found for the mechanical properties as all fracture parameters in the TL system for oak and ash are closer together than in the RL system.

The necessity of a reinforcement of the wood by the ray tissue seems to be explainable by taking the loading conditions of the living tree into consideration. As far as each growth ring consists of a less stiff earlywood and a latewood with a higher stiffness, these composite layers are forced by shear stresses during bending of the entire stem caused mainly by wind loads. The rays act as stiff pins preventing the layers of different stiffness from slipping of each other [26]. Our results indicate that even when microcracks have been developed already, the occurrence of a propagating macrocrack in the tangential plane is hindered by the ray tissue.

Therefore, one can conclude that the rays play an important role in the sophisticated structure of wood. Not only the mechanical properties but also the fracture mechanical properties are influenced by the ray tissue distinctly. Having the physiological importance of rays in mind the rays can be considered as a multifunctional tissue in the living tree.

References

1. H. HÖRIG, *Ing.-Arch.* **6** (1935) 8.
2. *Idem.*, *ibid.* **8** (1937) 1.
3. L. J. GIBSON and M. F. ASHBY, "Cellular solids. Cambridge Solid State Sci. Ser.," 2nd ed. (Cambridge University Press, Cambridge, 1997).
4. K. J. NIKLAS, "Plant Biomechanics" (Chicago University Press, Chicago, 1992).
5. E. KAHLE and J. J. WOODHOUSE, *J. Mater. Sci.* **29** (1994) 1250.
6. I. BURGERT and D. ECKSTEIN, *Trees* **15** (2001) 168.
7. Y. KAWAMURA, *Mokuzai Gakkaishi* **30** (1984a) 201.
8. *Idem.*, *ibid.* **30** (1984b) 785.
9. E. BADEL and P. PERRÉ, *Ann. For. Sci.* **56** (1999) 467.
10. I. BURGERT, A. BERNASCONI and D. ECKSTEIN, *Holz Roh- Werkst.* **57** (1999) 397.
11. I. BURGERT, A. BERNASCONI, K. J. NIKLAS and D. ECKSTEIN, *Holzforschung* **55**, in press.
12. W. H. BEERY, G. IFJU and E. MCLAIN, *Wood Fiber Sci.* **15** (1983) 395.
13. A. P. SCHNIEWIND, *Forest Prod. J.* **9** (1959) 350.
14. E. K. TSCHEGG, Equipment and Appropriate Specimen Shape for Tests to Measure Fracture Values (in German), Patent AT-390328 (1986).
15. H. HARMUTH, *Theor. Appl. Fract. Mech.* **23** (1995) 103.
16. S. E. STANZL-TSCHEGG, D. M. TAN and E. K. TSCHEGG, *Wood Sci. Technol.* **29** (1995) 31.
17. *Idem.*, *Int. J. Fract.* **75** (1996) 347.
18. A. REITERER, S. E. STANZL-TSCHEGG and E. K. TSCHEGG, *Wood Sci. Technol.* **34** (2000) 417.
19. H. SCHACHNER, A. REITERER and S. E. STANZL-TSCHEGG, *J. Mater. Sci. Lett.* **19** (2000) 1783.
20. P. NIEMZ, "Physik des Holzes und der Holzwerkstoffe" (DRW-Verlag, Leinfelden-Echterdingen, 1993).
21. R. WAGENFÜHR, "Holzatlas" (Carl Hanser Verlag, Leipzig, 2000).
22. H. HARMUTH, K. RIEDER, M. KROBATH and E. K. TSCHEGG, *Mat. Sci. Eng.* A **214** (1996) 53.
23. R. L. YOUNGS, U.S. For. Prod. Lab., Madison, Wis. Rept 2079 (1957).
24. M. GOULET, *Holz Roh- Werkst.* **18** (1960) 325.
25. D. FENGEL and G. WEGENER, "Wood—Chemistry, Ultrastructure, Reactions" (Walter de Gruyter, Berlin, New York, 1989).
26. C. MATTHECK and H. KUBLER, "Wood—the Internal Optimization of Trees" (Springer-Verlag, New York, 1995).

Received 9 April
and accepted 22 October 2001